Environmental Conditions Associated with Amazonian Squall Lines: A Case Study

JÚLIA C. P. COHEN

Department of Meteorology, Federal University of Pará, Belém, Brazil

MARIA A. F. SILVA DIAS

Department of Atmospheric Sciences, University of São Paulo, São Paulo, Brazil

CARLOS A. NOBRE

Center for Weather Forecasting and Climate Studies, National Institute for Space Research, São José dos Campos, Brazil

ABSTRACT

The environmental conditions associated with squall lines (SL) that were observed during the period of 13 April–13 May 1987 (GTE/ABLE-2B) originating at the northern coast of South America and propagating over the Amazon Basin are documented. The SL observed on 5–7 May are examined in more detail. The SL days had in common a stronger and deeper low-level jet when compared with the days without SL. Two possible explanations are found for the intensification of the low-level jet: propagating easterly waves in the tropical Atlantic, which eventually reach Manaus, and localized heat sources in the western Amazon. Both were observed on 5–6 May. It is suggested that numerical simulations should be performed to unravel the relative importance of each large-scale mechanism.

1. Introduction

Narrow bands of convective cloudiness over the northern coast of South America, from Guiana to the state of Maranhão in Brazil, are often identified in satellite imagery. Some of the narrow convective bands move inland as squall lines, others dissipate near the coast. According to Kousky (1980), the propagating and nonpropagating lines are basically initiated by the sea-breeze circulation.

During April and May 1987, several convective systems were observed over the Amazon region. Greco et al. (1990) and Garstang et al. (1994) investigated the evolution and morphology of these convective systems, which occurred during the Global Tropospheric Experiment/Amazon Boundary Layer Experiment (GTE/ABLE 2B). Details of the experimental design may be found in Harriss et al. (1990); Fig. 1 has the main geographical features of the Amazon region. Greco et al. (1990) classified three main types of organized convective systems: coastal occurring systems (COS), ba-

sin occurring systems (BOS), and locally occurring systems (LOS). The COS are large mesoscale to synoptic-scale systems of generally linear orientation that form along the northern coast of Brazil during the afternoon and travel across the basin as squall lines. These systems have been called "Amazon coastal squall lines" by Garstang et al. (1994) and Greco et al. (1994). According to these authors, the period of 21 April–3 May was dominated by COS, with 89% of the total rain over the central Amazon Basin (mesoscale network) produced on the eight COS days.

Sun and Orlanski (1981a) evaluated the mechanism of propagation of tropical squall lines using a linear model where the sea-breeze circulation produced a propagating wave associated with the trapeze instability produced by the diurnal oscillation of the boundary layer temperature profile. They obtained periods of the order of 1 day in some cases. An evaluation of the mechanisms responsible for the squall-line propagation at the Amazon region was carried out, also, by Silva Dias and Ferreira (1992) through the application of a linear spectral model with a wave-CISK parameterization of convection. They showed that in order to obtain group velocities associated with unstable modes with speeds similar to observed ones in the Amazon, the model had to be initiated with a vertical wind profile with a deep low-level easterly jet, which had been observed in squall-line days or COS days.

Corresponding author address: Dr. Maria A. F. Silva Dias, Departmento de Ciencias Atmosfericas, Instituto Astronomico e Geofisico, Universidade de São Paulo, Rua do Matao 1226, 05508-900 São Paulo SP, Brazil.
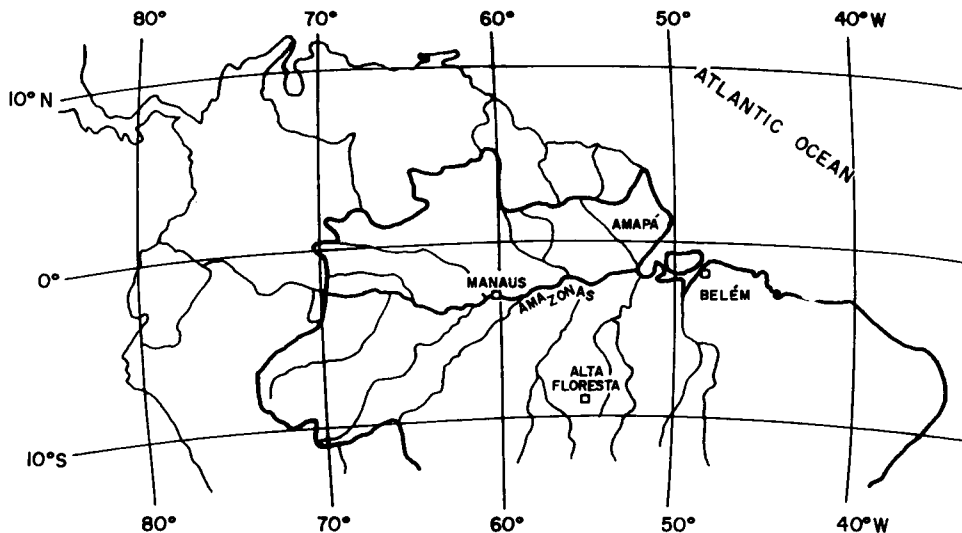E-mail: mafdsdia@model.iag.usp.br

FIG. 1. Map of the Amazon Basin of Brazil showing main geographical features.

In the present study, we document the environmental conditions associated with the squall lines, which passed through the data network of ABLE-2B during the period of 13 April–13 May 1987. This work is divided into two parts: first we examine the average wind profile in different convective evolutions originating at the northern coast of Brazil, then we present a case study of the 5–7 May squall line. The local conditions associated with the 6 May squall line were documented by Scala et al. (1990), Garstang et al. (1994), and Greco et al. (1994); here the focus will be on the environmental conditions associated with this system.

2. Data

The squall lines originating from the northern coast of South America from 13 April to 13 May 1987 have been observed in hourly GOES-E images. From these images, the lifetime, speed, and distance of inland propagation were determined. These systems were classified according to their inland propagation as CLC—coastal line of convection, which moved no more than 170 km inland; SL1—squall-line type 1, which moved between 170 and 400 km inland; and SL2—squall-line type 2, which moved more than 400 km inland. The same classification was used in Cohen et al. (1989). The threshold of 170 km was chosen because it corresponds to the average width of the squall line as seem from satellite infrared images.

The ABLE-2B radiosonde network consisting of five sites around the borders, and one in the center, of the Brazilian Amazon has been used. The soundings were released at 0000, 0600, 1200, and 1800 UTC (see Fig. 3 in Harriss et al. 1990). The equivalent potential temperature and water vapor mixing ratio have been calculated for every sounding.

The ECMWF analysis datasets for the period of 4–6 May 1987 have been used to describe the large-scale environment associated with the squall-line occurrence of 5 and 6 May 1987.

3. Climatology of squall lines

According to Cohen et al. (1989), 268 cases of squall lines were observed during the period 1979–86,

TABLE 1. Distribution of squall lines during GTE/ABLE 2B.

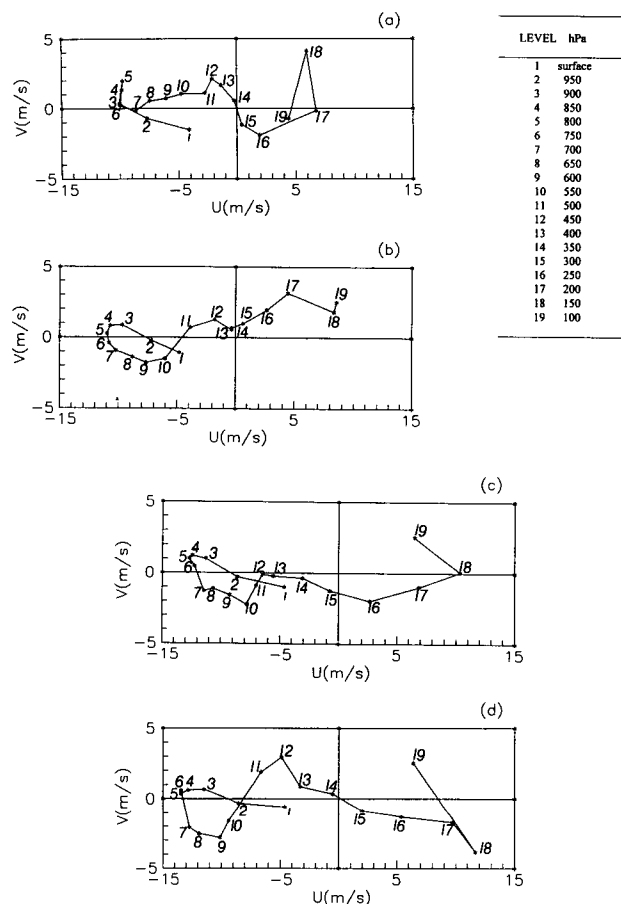| Date	Category	V (m s^{-1})
16 April	CLC	—
17 April	SL2	20.0
18 April	SL2	18.9
20 April	SL2	12.5
21 April	SL2	16.4
22 April	SL2	12.8
23 April	SL2	*
24 April	SL2	10.7
25 April	SL2	13.7
26 April	SL1	19.7
27 April	CLC	—
28 April	CLC	—
29 April	SL2	13.0
30 April	SL2	12.8
4 May	CLC	—
5 May	SL2	14.4
6 May	SL2	18.1
7 May	SL2	16.8
8 May	SL2	17.3
9 May	CLC	—
10 May	SL2	12.4
11 May	SL2	20.5
12 May	CLC	—
13 May	CLC	—

* Not possible to estimate V.

FIG. 2. Average wind hodograph over Belém at 1200 UTC (0900 local time) for different situations that occurred during GTE/ABLE 2B: (a) absence of convective line; (b) for day with coast line convective (CLC); (c) formation of squall line (SL); (d) for the period from 20 through 26 April.

originating at the northern coast of Brazil. From these, 62% were classified as CLC, 11% as SL1, and 27% as SL2. The frequency of these systems (CLC, SL1, and SL2) is larger between April and August. With respect to SL2, the maximum frequency occurs in July. These systems thus have a preference for the dry season when the diurnal convection over the Amazon Basin is suppressed.

The average propagation speed of SL1 and SL2 were 12 and 16 m s^{-1}, respectively, which is similar to the speeds observed in other tropical regions. Molion (1987) estimated that the average propagation speed of squall lines over the Amazon Basin was 10° of longitude per day (12.8 m s^{-1}). According to Fernandez (1982), the average speed of squall lines is 14.8 m s^{-1} over West Africa and 14.6 m s^{-1} over the tropical Atlantic. In Venezuela, the squall lines show average speeds of 13 m s^{-1} (Fernandez 1980).

The average lifetime of CLC, SL1, and SL2 is 9, 12, and 16 h, respectively (Cohen et al. 1989). These life-

times are similar to the ones observed in the Gulf of Carpentaria (Australia), which are of 12–24 h (Drosdowsky and Holland 1987). The average lifetime of the squall lines over West Africa is 39.7 h, while the average lifetime over the Atlantic is 9.7 h (Fernandez 1982). The squall lines at Venezuela have an average lifetime of 3.5 h (Fernandez 1980; Betts et al. 1976).

The maximum displacement observed for a SL2 was of the order of 2000 km. According to Fernandez (1982), the average displacement of the squall lines at West Africa is 2100 km, while in Venezuela it is about 150 km (Betts et al. 1976). Thus, the Amazonian squall lines travel from the coast well into the Amazon Basin, having an impact on the local precipitation in the dry season.

The region of the squall-line formation is between 10°N and 5°S. Cavalcanti (1982) observed that the extreme points of the squall lines follow the displacement of the ITCZ: squall lines are usually south of the ITCZ. The squall lines in West Africa have similar behavior but with opposite symmetry to the ITCZ, which was located to the north of the equator during GATE (Fernandez 1982).

Cavalcanti (1982) observed that the maximum number of squall lines occurred when the ITCZ was well established without considering the propagation inland. Cohen et al. (1989) concluded that the SL2 type is more frequent when the ITCZ is very well established and SL1 does not seem to depend on the ITCZ condition, although there was a smaller number of SL1 cases that might be the cause of this apparent independence.

The majority of the squall lines studied by Cohen et al. (1989) showed lengths between 700 and 1900 km, while the width was between 100 and 220 km; the average dimensions were of the order of 1400 km in length and 170 km in width. The average dimensions of the squall lines in Africa are 750 km in length and 433 km in width. On the other hand, the average length and width of the squall lines in Venezuela are 98 and 29 km, respectively (Betts et al. 1976).

In summary, Amazonian squall lines are large mesoscale systems that occur mainly in the dry season of the Amazon Basin, propagate as fast as other observed tropical squall lines, and live as long as squall lines observed in Australia but less than the West African squall lines. The Amazonian squall lines live longer than the ones observed in the Atlantic and in Venezuela.

4. Squall lines during the ABLE-2B

The squall lines that were observed during the ABLE-2B are listed in Table 1, where CLC corresponded to 22.6% of the cases, SL1 occurred only once, and SL2 corresponded to 51.6% of the cases. A sequence of consecutive days of squall-line formation was observed from 20 to 26 April; the first six days correspond to SL2 cases, and the last day to a SL1 case. From here on we will refer to SL1 and SL2 as SL cases.

(a)

MCT/INPE-CP GOES-7 87-125 18:00

(b)

MCT/INPE-CP GOES-7 87-126 00:00

(c)

MCT/INPE-CP GOES-7 87-126 06:00

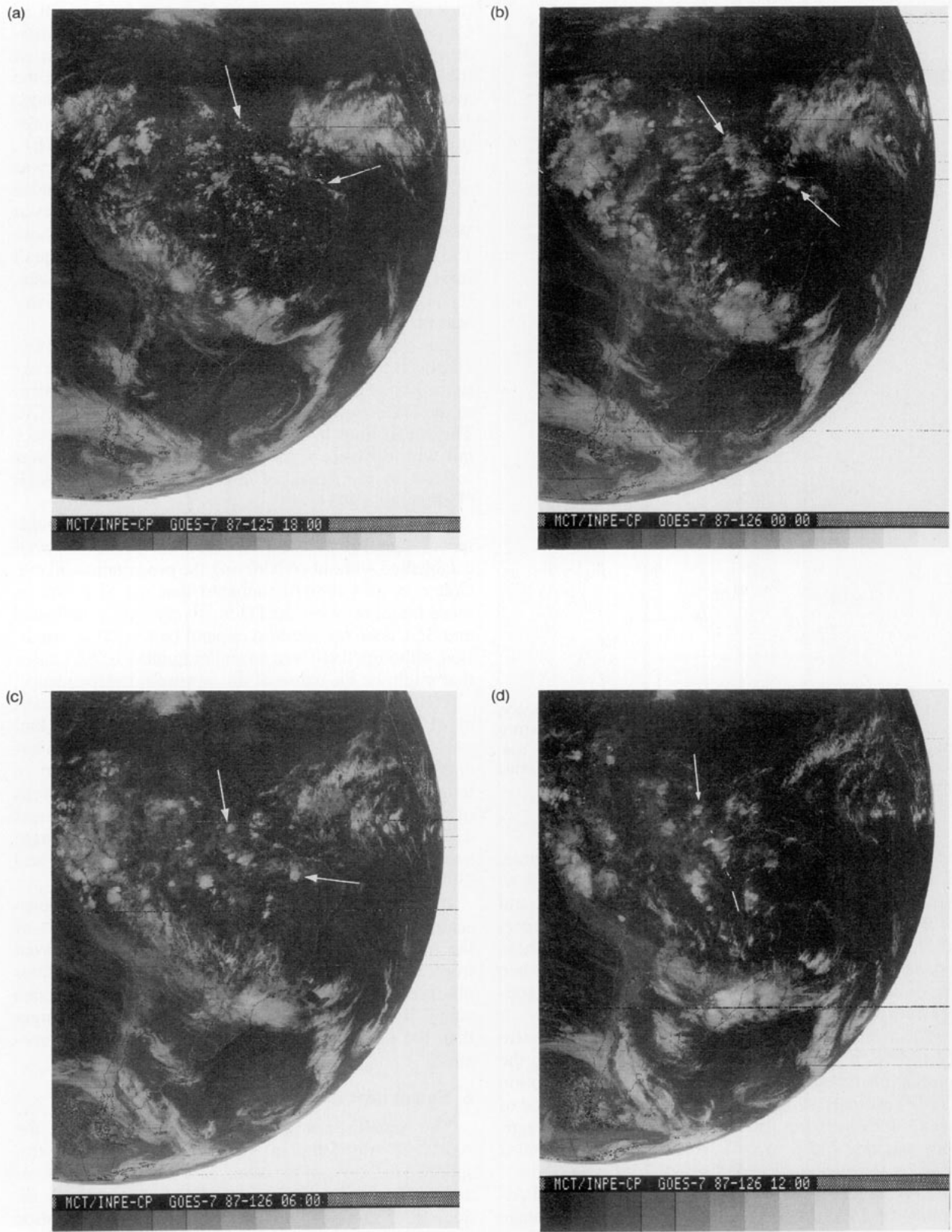(d)

MCT/INPE-CP GOES-7 87-126 12:00

FIG. 3. Satellite images from GOES-East on the infrared channel for the period from 5 to 7 May 1987: (a) 1800 UTC 5 May; (b) 0000 UTC 6 May; (c) 0600 UTC 6 May; (d) 1200 UTC 6 May; (e) 1800 UTC 6 May; (f) 0000 UTC 7 May; (g) 0600 UTC 7 May; (h) summary of the leading edge position of the squall line.
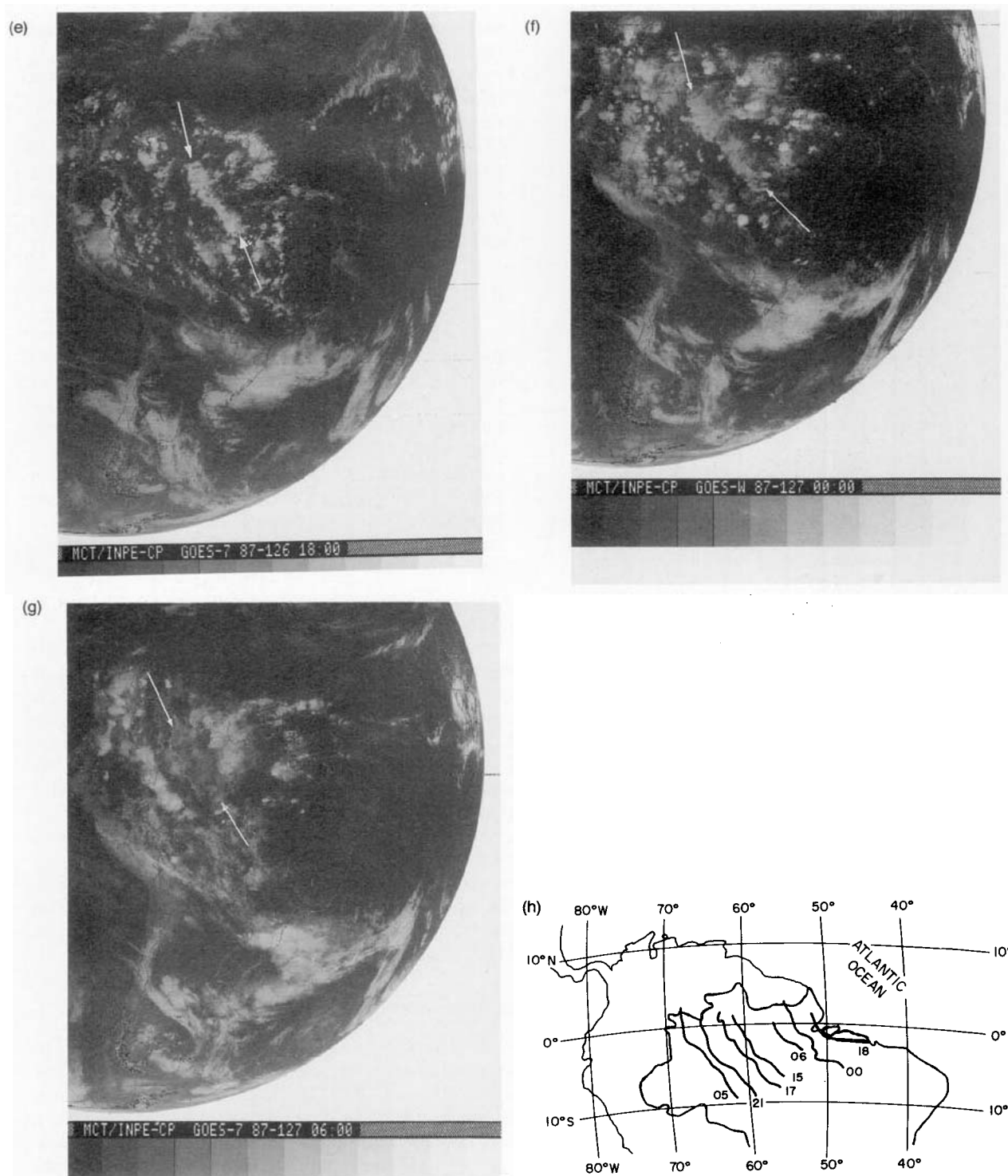
FIG. 3. (*Continued*)

The convection associated with the formation of the squall line along the coast is initiated around or after local noon. A morning sounding at the city of Belém, which is located 100 km from the coast, may be con-sidered representative of the environmental conditions, prior to squall-line formation. Figure 2 shows the average wind hodographs for the 1200 UTC sounding (0900 local time) for the following conditions: (a) ab-
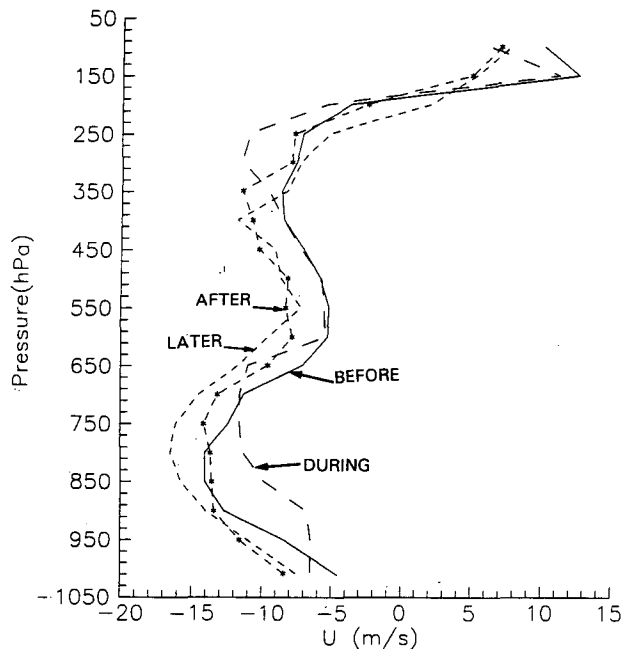
FIG. 4. Vertical profile of the zonal wind for different stages of the SL over Belém.

sence of convective lines; (b) formation of CLC; (c) formation of SL; and (d) for the period from 20 through 26 April.

The maximum average zonal wind (easterly low-level jet) occurred around 800 hPa in all cases. The low-level jet associated with the VIMHEX squall lines had a speed of 11.8 m s^{-1} and was located 2.8 km above the surface (Fernandez 1980). The easterly jet was stronger in days with SL than in days without SL or in days with CLC. In all situations there is a layer containing almost constant wind velocity, around the maximum; the thickness of this layer varies in the different situations. In the absence of convective lines, this layer is between 900 and 750 hPa; for the CLC case, between 900 and 700 hPa; and for SL, between 900 and 650 hPa, and the same for the seven squall-line days. Garstang et al. (1994) showed that the wind maximum in the central Amazon Basin for three SL cases was located in the 650–850-hPa layer.

The wind direction at 850 hPa was more parallel to the coast in days without convective lines than in days with squall lines but was almost similar in days with CLC and SL (Figs. 2b,c). According to Kousky (1980), once the cumulonimbi are well developed along the sea front, at the northern coast of South America, the line of convective activity may continue to propagate inland on its own, possibly as a squall line. He noted, in one case, that the sea-breeze front penetrated well into the continent where the mean flow was onshore (north of the mouth of the Amazon River) and only slightly into the continent where the mean flow

was more parallel to the coast or even slightly offshore (east-southeast of the mouth of the Amazon).

In the present case the wind direction with respect to the coast did not appear to be an important element for the squall-line propagation as suggested by Kousky (1980). Thus, we point out in agreement with the results of Silva Dias and Ferreira (1992) that the magnitude of the wind speed and the thickness of the low-level jet are important elements for the inland propagation of SL.

5. Case study

The 5 May 1987 squall line was first observed near the northern coast of Brazil at 1800 UTC (1500 local time), as may be seen in Fig. 3, which shows its life history. This SL moved inland (0000 UTC 6 May), and by 0600 UTC 6 May the convective activity is somewhat weaker than in the previous images. This condition remained until local noon when the SL was reinforced, as may be seen also by 1800 UTC. A few hours later the length of the SL was almost double with relation to its initial dimension along the coast. The SL's dissipation was initiated during the following night. The lifetime of this system was close to 36 h. Figure 3h shows a summary of the squall line's leading edge position throughout its lifetime.

According to Molion (1987), the reduction of the thermal forcing during the night induces the dissipation of cloudiness associated with the squall lines in the Amazon; convective activity may be enhanced again in the following day when the surface heating is established. However, there were cases in which it was observed that the dissipation occurred in hours of heating (Cohen et al. 1989). It was also noted that the regeneration of the SL occurs often in the northern portions of the Amazon region during nighttime. This may indicate a possible influence of topography in the region (in northwestern Pará and western Amapá), which reaches heights between 200 and 500 m above sea level.

a. Large-scale wind structure

The vertical profiles of zonal wind in Belém may be seen in Fig. 4 for the following stages of the SL: before its formation (1200 UTC), close to its passage over Belém (1800 UTC), after leaving Belém (0000 UTC), and later on (0600 UTC). The magnitudes of the easterly jet were the same before formation and after the passage of the SL (−14.1 m s^{-1}), which correspond to the propagation speed of this SL on the first day (see Table 1). The jet slowed down by 1800 UTC when the SL was over Belém but shows larger intensities later on (16.5 m s^{-1}) when compared to the previous stages. Betts et al. (1976) observed during the VIMHEX the increase in wind speeds in lower and upper levels after the passage of the squall lines over Venezuela; how-
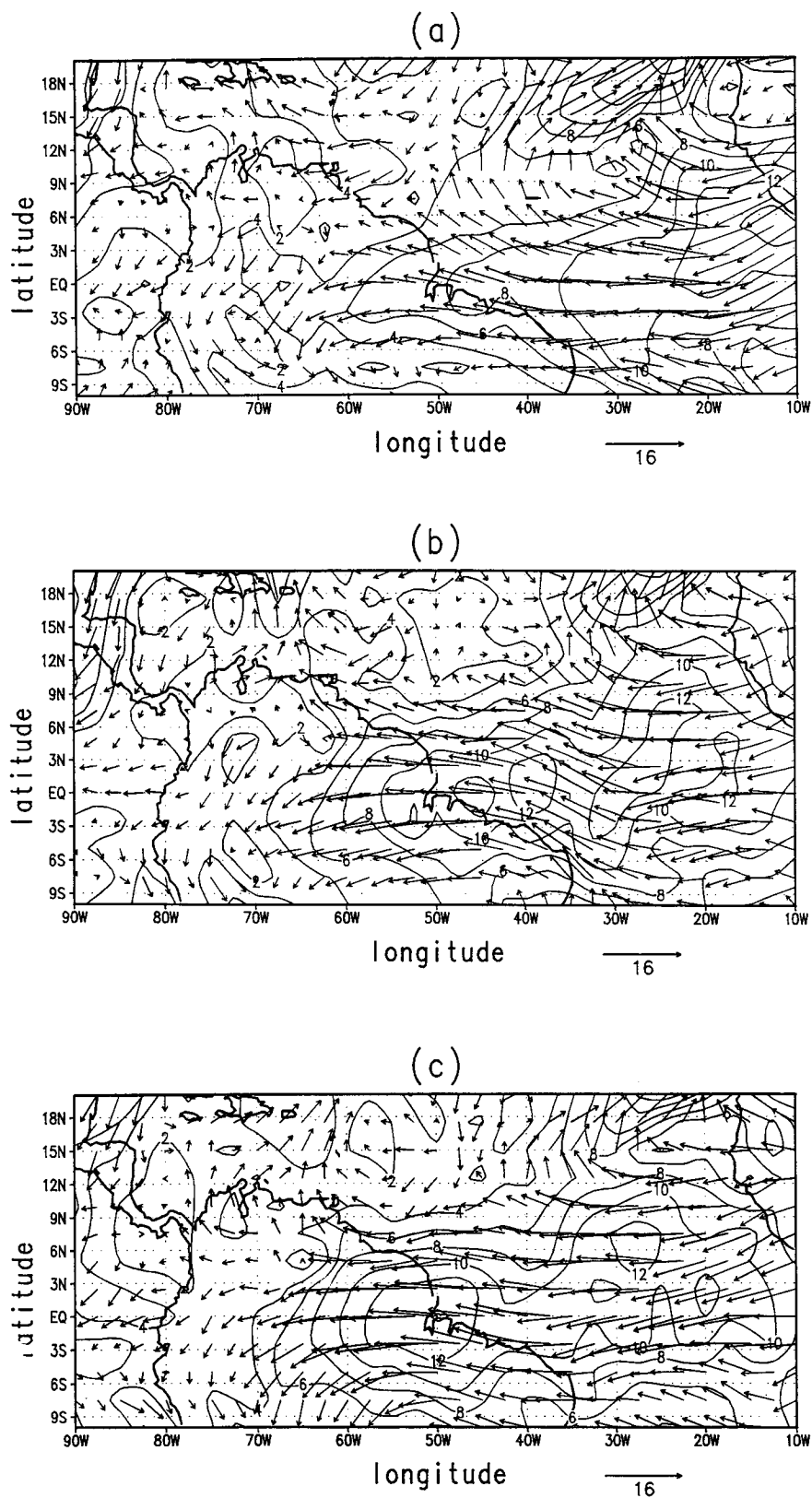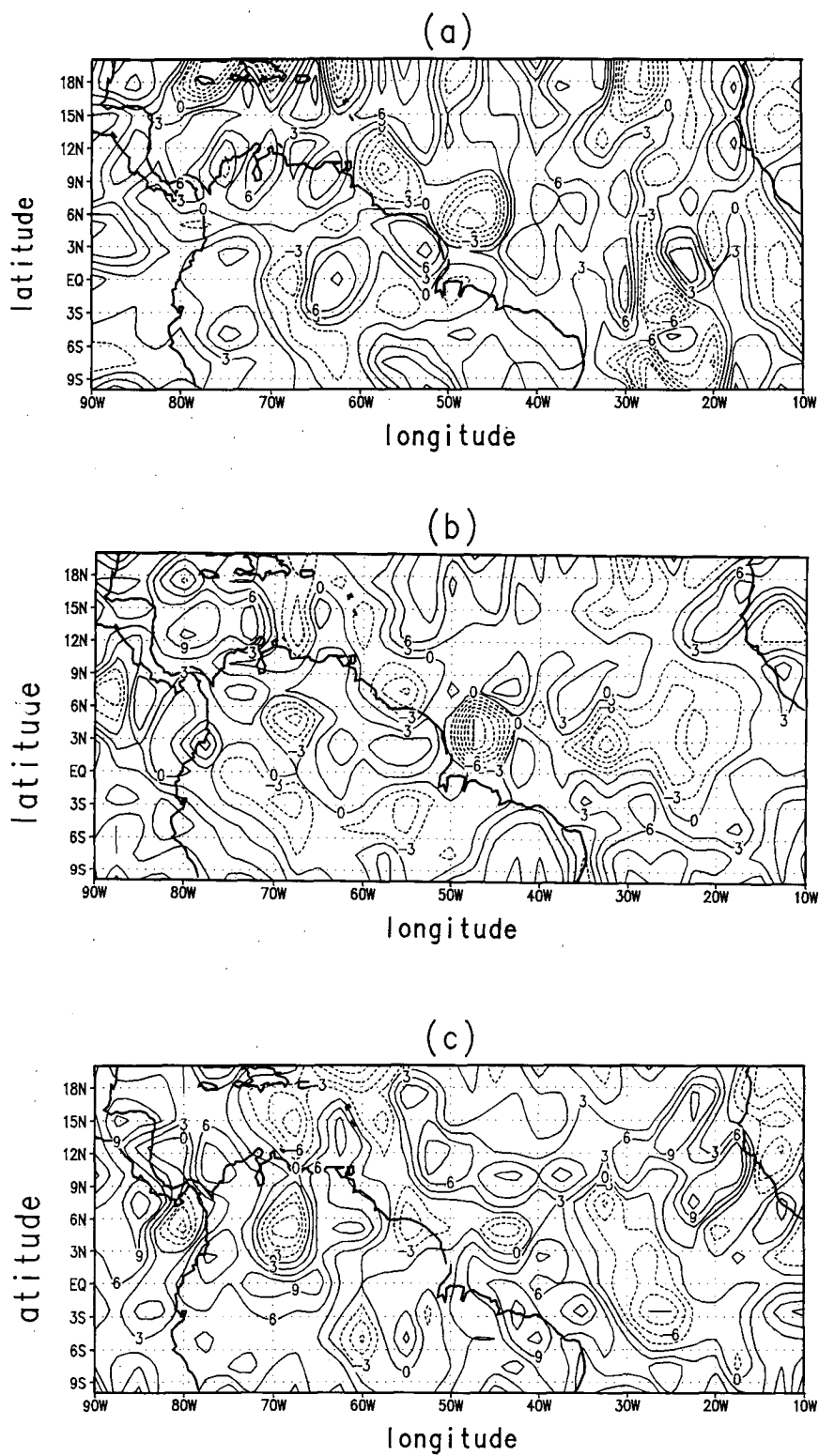
FIG. 5. Horizontal structure of the wind and isotachs (m s^{-1}) at 700 hPa for the following days: (a) 4 May, (b) 5 May, and (c) 6 May at 1200 UTC.

FIG. 6. Vertical component of the wind (Pa s^{-1}) at 500 hPa for the following days:
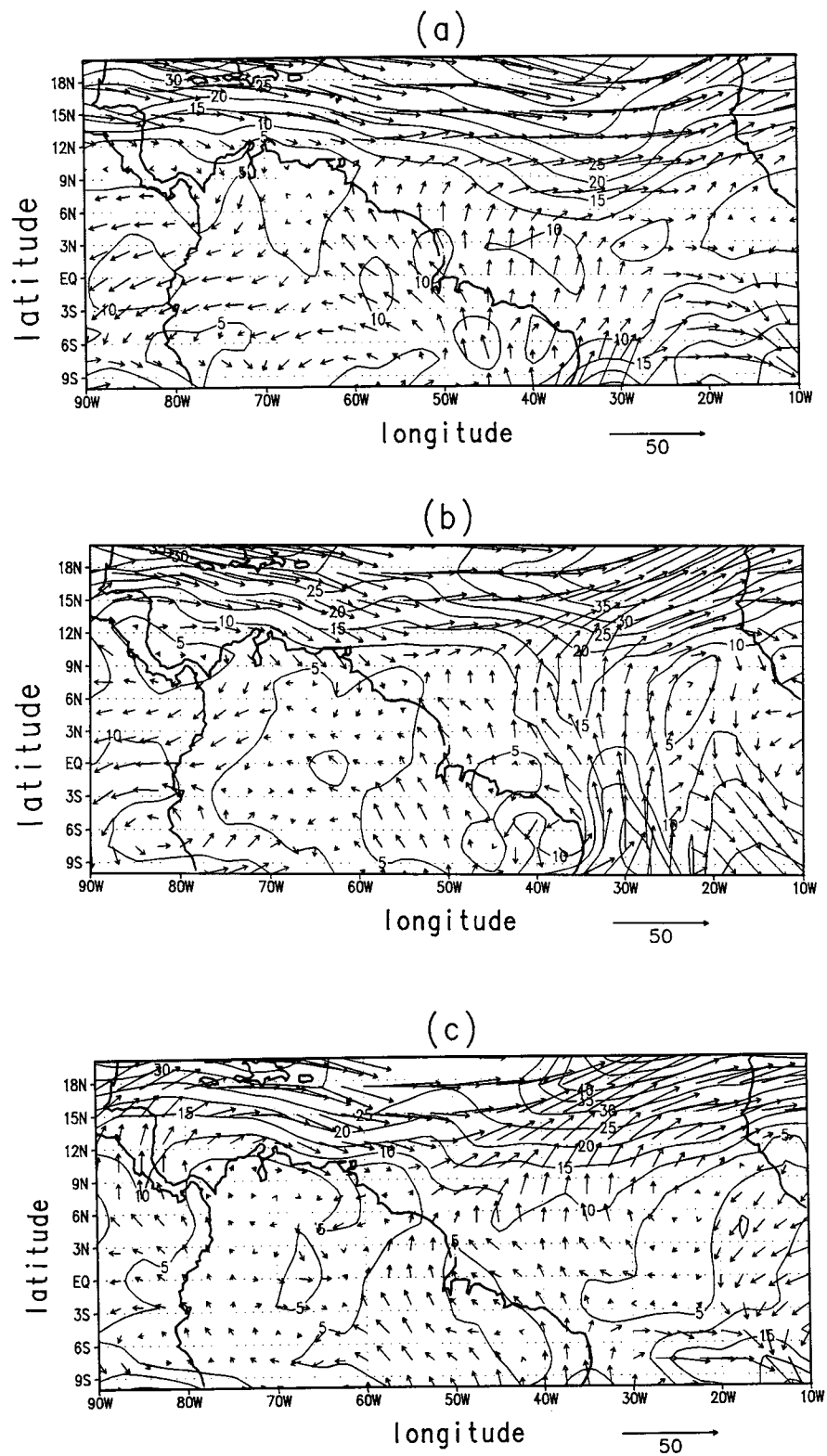(a) 4 May, (b) 5 May, and (c) 6 May at 1200 UTC.

FIG. 7. Horizontal structure of the wind and isotachs (m s^{-1}) at 200 hPa for the following days: (a) 4 May, (b) 5 May, and (c) 6 May at 1200 UTC.
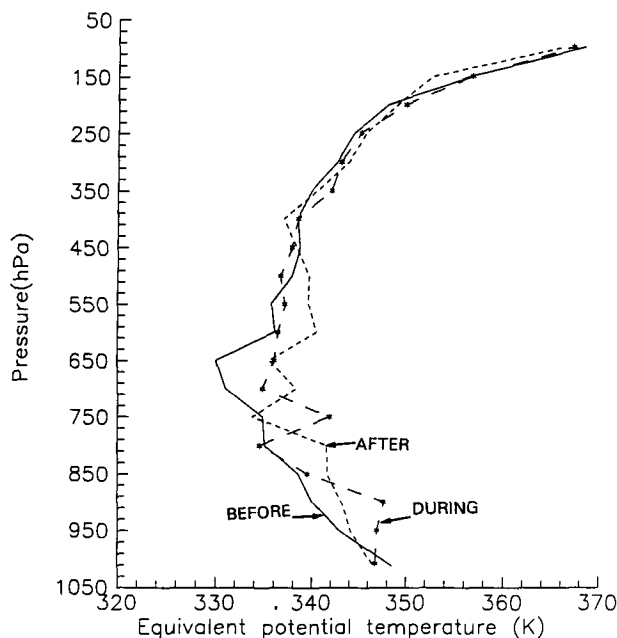
FIG. 8. Vertical profile of the equivalent potential temperature at Belém for differents stages of the SL.

Silva Dias et al. (1983) showed that a localized equatorial heat source, of the order of or larger than the equatorial Rossby radius of deformation (~1500 km), produces an organized response in a scale much larger than the source. In their model, an enhancement of the upper-level westerlies and low-level easterlies is produced to the east of the equatorial source.

Figure 5 shows the horizontal structure of the wind and its isotachs at the 700-hPa level for a period of 3 days at 1200 UTC. As shown in Table 1, 4 May was a CLC case but is included here to represent the large-scale situation 1 day before the SL case under study.

Figure 5 shows strong winds along a belt close to the equator from 10° to 70°W during these 3 days. Along the northern coast between 40° and 50°W the wind accelerates from 4 May to 5 May and to 6 May. The environmental flow before the beginning of the SL case (Fig. 5b) shows several maxima in speed from the eastern boundary of the figure until the Amazon region coastal region. In the following day (6 May) there is a well-defined wind maximum close to the coast. The change in sign of the meridional component may be seen in the Atlantic similar to the one detected in GATE easterly waves by Reed et al. (1977), more intense on 5 May, and similar to the one detected by Kagano (1979) at Manaus also associated with easterly waves.

Figure 6 depicts the vertical velocity field for the same 3 days at the 500-hPa level; local maximum in the negative values indicates, if associated with cloudiness in the satellite infrared images, the presence of strong convective activity, the so-called localized heat source. Comparing Fig. 6b and Fig. 3a, we see that heat
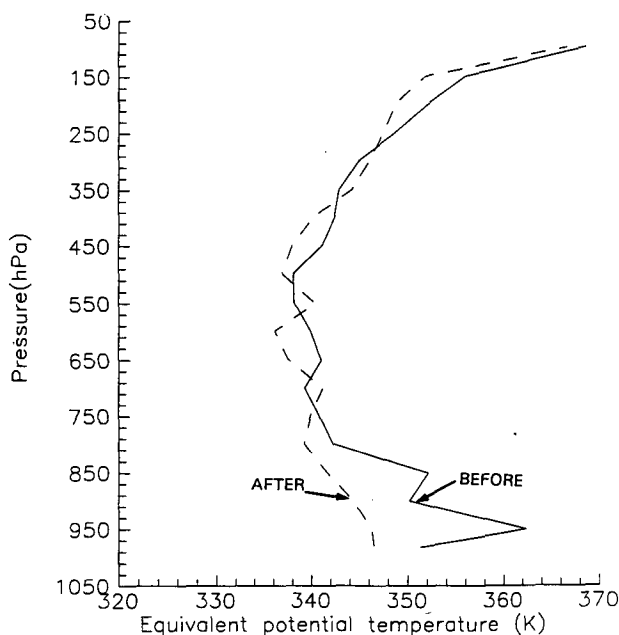
ever, the soundings were closer in time than in the present case. Scala et al. (1990) show the surface wind speeds recorded by a PAM network close to Manaus showed that surface gust winds associated with the 6 May squall line were of the order of 10 m s⁻¹ and lasted only a few minutes.

The thickness of the layer with maximum zonal wind was of almost constant magnitude in the four radiosondes in Fig. 4 corresponding to the different stages of the SL. However, at 1800 UTC this layer is lifted, returning to the initial levels in later times.

As mentioned previously, the magnitude of the easterly low-level jet was stronger in days with SL than in other situations. To evaluate the causes for the stronger winds in SL days, we will present the synoptic features associated with this SL. Reviewing the work in the literature, we focus on two possible large-scale mechanisms that may produce an intensification of the low-level jet observed in SL days: easterly waves and tropical heat sources.

Reed et al. (1988) examined the ability of the current ECMWF data assimilation system to detect and predict easterly waves over the tropical Atlantic. They identified 20 easterly waves in a 2-month period. Wave characteristics were similar to those reported in earlier studies: wavelengths were typically in the 2000–3000-km range, periods in the 3–5-day range, and phase speeds between 6° and 7° of longitude per day. Kagano (1979) analyzed daily radiosonde data for Manaus and Belém and noticed periodic changes in wind direction and relative humidity at low levels. These oscillations showed a period of 3–5 days, typical of easterly waves.

FIG. 9. Vertical profile of the equivalent potential temperature at Alta Floresta for differents stages of the SL.

sources are located in the Atlantic between 35° and 20°W and in the western side of the Amazon region at 67°W between 6°N and 6°S. The winds 700 hPa (Fig. 5) intensify in response to the heat source in the western Amazon and are seen to converge just east of the Andes. The 200-hPa wind field in Fig. 7 shows two anticyclonic vortices, one at each side of the equator along 80°W, associated with the low-level convergence of the heat source. The westward tilt with height of the convergence–divergence pattern is a common feature associated with tropical heat sources (e.g., Horel et al. 1989).

In summary, the synoptic situation includes the presence of easterly waves and also of a localized heat source. Each one of these features may be responsible, on its own, for the acceleration of the low-level jet. It is also possible that propagation characteristics of waves originated along the Atlantic coast may be significantly changed by localized heat sources over western Amazon. The role of each should be investigated further, through numerical simulations, to evaluate their relative importance.

b. Thermodynamic structure

The vertical profile of equivalent potential temperature associated with the squall-line passage over Belém and Alta Floresta may be seen in Figs. 8 and 9, respectively. This latter station has been included because it is farther inland and away from the direct influence of the sea-breeze circulation. The SL passed over Belém at 1800 UTC 5 May and over Alta Floresta at 2100 UTC 6 May. The profiles in Figs. 8 and 9 are labeled before, during, and after with respect to the time of the squall-line passage over each location. The radiosonde launched at 1200 UTC 6 May 1987 represents the condition before the passage of the SL over Alta Floresta, and the period after SL is represented by the radiosonde launched at 0000 UTC 7 May 1987. There is a considerable difference in the evolution of the equivalent temperature profile in the two locations. In Alta Floresta (Fig. 9), after SL passage the sounding shows a decrease of equivalent potential temperature below 750 hPa and a more mixed structure than in the before passage basically due to the effect of downdrafts. This is in agreement with the evolution noted by Houze (1977), for GATE squall lines; Chong et al. (1987), for COPT81; Garstang et al. (1994), for GTE/ABLE 2B squall lines; among others, although the time interval between soundings was shorter in these studies than in the present case. The evolution in Belém (Fig. 8) shows a different situation: there is an increase in the equivalent potential temperature below 600 hPa from the before sounding to the during and after soundings. This is indeed a result of moistening of this level that may be due to the arrival of the coastal air mass behind the sea-breeze front.

6. Summary and conclusions

We have documented the features of the environmental wind profile that were associated with the occurrence of squall lines during the period of 13 April–13 May 1987, during GTE/ABLE 2B. The squall lines formed along the northern coast of South America and propagated inland over the Amazon region. The main feature associated with squall-line days was the magnitude and thickness of the low-level jet, which had been also reported by Silva Dias and Ferreira (1992). In a case study of the 5 and 6 May squall line we look for possible large-scale mechanisms that might explain a deeper and stronger low-level easterly jet. We find that easterly waves were present over the Atlantic Ocean and approached the northern coast of South America on 5 May. However, the presence of a localized heat source in the western Amazon is seen to increase in strength from 4 May to 5 and 6 May and the low-level winds are seen to converge to that region. We conclude that the combination of both mechanisms was present in this case and only through numerical simulations may the relative importance of each be established. We have also examined the evolution of the vertical profile of equivalent potential temperature at two locations and have seen that when removed from the direct influence of the sea-breeze circulation the evolution is typical of the effect of downdrafts also reported in other studies. The evolution close to the coast is dominated by the advection of moisture produced by the sea breeze.

The squall lines that propagate over the Amazon region may be seen as a complex system where scale interactions range from the large-scale environmental characteristics, to the mesoscale and cloud-scale circulations. In the larger scale, important features are the propagation of easterly waves in the Atlantic and the presence of tropical heat sources in the western Amazon. In the mesoscale the sea-breeze formation and evolution plays a fundamental role, while the cloud-scale circulations maintain the squall-line propagation in a quasi-steady state for lengths of over 1000 km and over 24 h. Although several numerical simulations have been performed for midlatitude squall lines in different environments (e.g., Rotunno et al. 1988; Schmidt and Cotton 1990; Cram et al. 1992; and others) and for a few cases of tropical environments (e.g., Nicholls et al. 1988; Hahmann 1992), there is a clear need for numerical studies where the three scales (large scale, mesoscale, and cloud scale) are properly treated for the particular case of propagating Amazon squall lines.

COLA (Center for Ocean–Land–Atmosphere). We acknowledge helpful discussions with Dr. Pedro L. Silva Dias.

REFERENCES

Betts, G. M., R. W. Grower, and M. W. Moncrieff, 1976: Structure and motion of the tropical squall lines over Venezuela. *Quart. J. Roy. Meteor. Soc.,* **102,** 395–404.

Cavalcanti, I. F. A., 1982: Um estudo sobre interações entre sistemas de circulação the escala sinótica e circulações locais. M.S. thesis, INPE-2494-TDL/097, São José dos Campos, São Paulo, Brazil, 113 pp.

Chong, M., P. Amayenc, G. Scialom, and J. Testud, 1987: A tropical squall line observed during the COPT 81 Experiment in West Africa. Part I: Kinematic structure inferred from dual-Doppler radar data. *Mon. Wea. Rev.,* **115,** 670–694.

Cohen, J. C. P., M. A. F. Silva Dias, and C. A. Nobre, 1989: Aspectos climatológico das linhas de instabilidade na Amazonia. *Climanalise, Boletim de monitoramento e analise climatica,* Vol. 4, INPE/CPTEC, 34–40.

Cram, J. M., R. A. Pielke, and W. R. Cotton, 1992: Numerical simulation and analysis of a prefrontal squall line. Part I: Observations and simulations results. *J. Atmos. Sci.,* **49,** 189–208.

Drosdowsky, W., and G. J. Holland, 1987: North Australian cloud lines. *Mon. Wea. Rev.,* **115,** 2645–2659.

Fernandez, W., 1980: Environmental conditions and structure of some types of convective mesoscales observed over Venezuela. *Arch. Meteor. Geophys. Bioklimatol.,* **A29,** 249–267.

——, 1982: Environmental conditions and structure of the West African and Eastern tropical Atlantic squall lines. *Arch. Meteor. Geophys. Bioklimatol.,* **A31,** 71–89.

Garstang, M., L. Massier Jr., J. Halverson, S. Greco, and J. Scala, 1994: Amazon coastal squall lines. Part I: Structure and kinematics. *Mon. Wea. Rev.,* **122,** 608–622.

Greco, S., and Coauthors, 1990: Rainfall and surface kinematic conditions over central Amazonia during ABLE 2B. *J. Geophys. Res.,* **95,** 17 001–17 014.

——, J. Scala, J. Halverson, H. L. Massie Jr., W. K. Tao, and M. Garstang, 1994: Amazon coastal squall lines. Part II: Heat and moisture transports. *Mon. Wea. Rev.,* **122,** 623–635.

Hahmann, A. N., 1992: Simulations of the Amazon Basin circulation using The Pennsylvania State University/National Center for Atmospheric Research Mesoscale Model. Ph.D. dissertation, University of Utah, 116 pp.

Harriss, R. C., and Coauthors, 1990: The Amazon boundary layer experiment: Wet season 1987. *J. Geophys. Res.,* **95,** 16 721–16 736.

Horel, J. D., A. N. Hahmann, and J. E. Geisler, 1989: An investigation of the annual cycle of convective activity over the tropical Americas. *J. Climate,* **2,** 1388–1403.

Houze, R. A., 1977: Structure and dynamics of a tropical squall line system. *Mon. Wea. Rev.,* **105,** 1540–1567.

Kagano, M. T., 1979: Um estudo climatológico e sinótico utilizando dados de radiossondagem de Manaus e Belém. M.S. thesis, INPE-1559-TDL/013, São José dos Campos, São Paulo, Brazil, 82 pp.

Kousky, V. E., 1980: Diurnal rainfall variation in the northeast Brazil. *Mon. Wea. Rev.,* **108,** 488–498.

Molion, L. C. B., 1987: On the dynamic climatology of the Amazon Basin and associated rain producing mechanisms. *Geophysiology of Amazonia Vegetation and Climate Interactions,* R. E. Dickinson, Ed., Wiley Series in Climate and the Biosphere; Wiley & Sons, 391–407.

Nicholls, M. E., R. H. Johnson, and W. R. Cotton, 1988: The sensitivity of two-dimensional simulations of tropical squall lines to environmental profiles. *J. Atmos. Sci.,* **45,** 3625–3649.

Reed, R. J., D. C. Norquist, and E. E. Recker, 1977: The structure and properties of African wave disturbances as observed during phase III of GATE. *Mon. Wea. Rev.,* **105,** 317–333.

——, A. Hollingsworth, W. A. Heckley, and F. Delsol, 1988: An evaluation of the performance of the ECMWF operational system in analyzing and forecasting easterly wave disturbances over Africa and the tropical Atlantic. *Mon. Wea. Rev.,* **116,** 824–865.

Rotunno, R., J. B. Klemp, and M. L. Weisman, 1988: A theory for strong, long-lived squall lines. *J. Atmos. Sci.,* **45,** 463–485.

Scala, J. R., and Coauthors, 1990: Cloud draft structure and trace gas transport. *J. Geophys. Res.,* **95,** 17 015–17 030.

Schmidt, J. M., and W. R. Cotton, 1990: Interactions between upper and lower tropospheric gravity waves on squall line structure and maintenance. *J. Atmos. Sci.,* **47,** 1205–1222.

Silva Dias, M. A. F., and R. N. Ferreira, 1992: Application of the a linear spectral model to the study of Amazonian squall lines during GTE/ABLE 2B. *J. Geophys. Res.,* **97,** 20 405–20 219.

Silva Dias, P. L., W. H. Schubert, and M. DeMaria, 1983: Large-scale response of the tropical atmosphere to transient convection. *J. Atmos. Sci.,* **40,** 2689–2707.

Sun, W. Y., and I. Orlanski, 1981a: Large mesoscale convection and sea breeze circulation. Part I: Linear stability analysis. *J. Atmos. Sci.,* **38,** 1675–1693.